Supplement for: Methoxy aromatic acids in an Arctic ice core from Svalbard: a proxy record of biomass burning

Mackenzie M. Grieman[1], Murat Aydin[1], Elisabeth Isaksson[2], Margit Schwikowski[3], and Eric S. Saltzman[1]

[1]Department of Earth System Science, University of California, Irvine, Irvine, California, 92697-3100, USA
[2]Norwegian Polar Institute Fram Centre Tromsø, NO-9296 Norway
[3]Laboratory of Environmental Chemistry, Paul Scherrer Institut, Villigen, Switzerland

Correspondence to: Mackenzie M. Grieman (mgrieman@uci.edu)

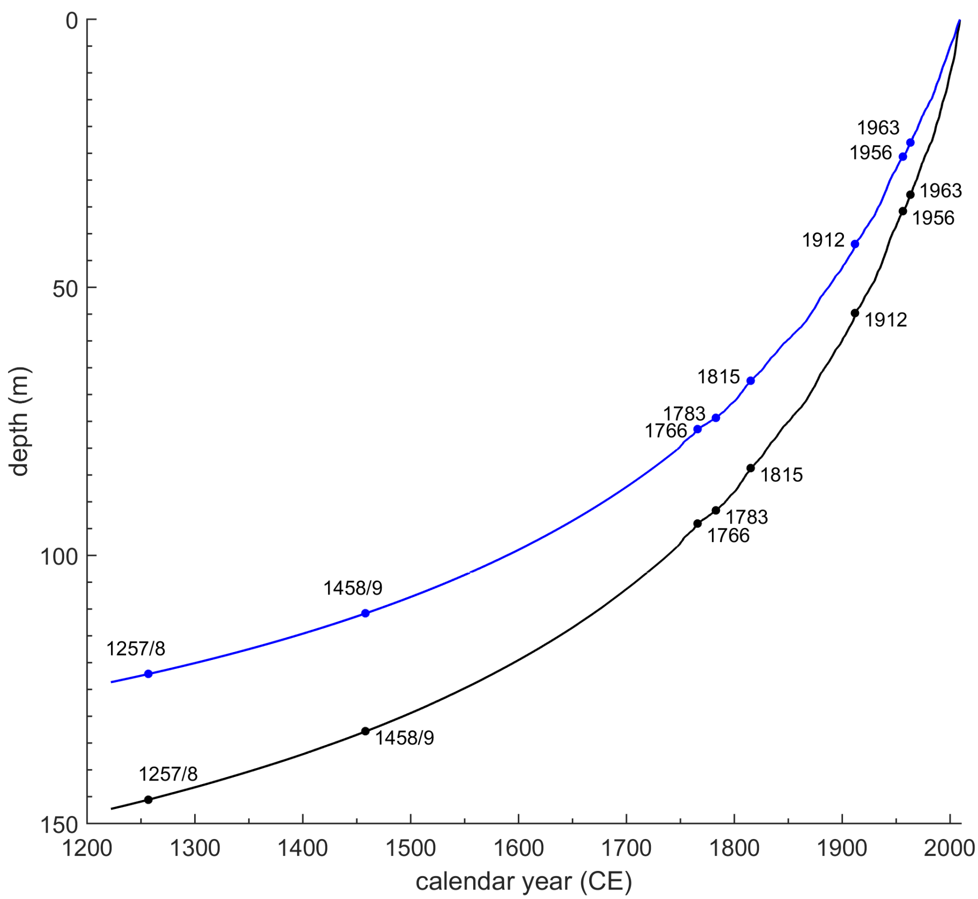

Figure S1. Lomonosovfonna ice core depth-age scale (adapted from Wendl et al., 2015). The black curve is the depth in meters. The blue curve is the depth in meters water equivalent. The points indicate tie points. These tie points are all volcanic eruptions, except for a tritium peak in 1963.

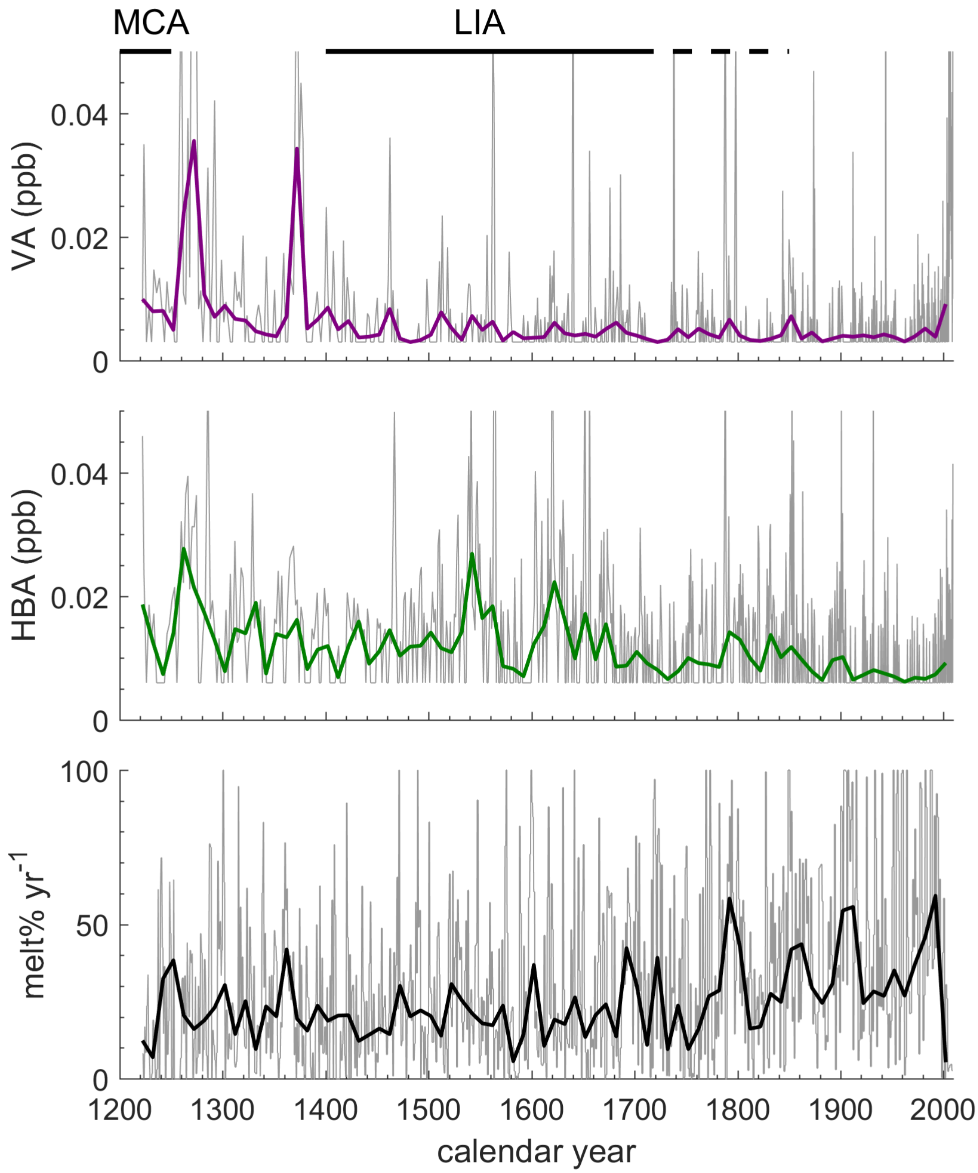

Figure S2. Lomonosovfonna melt layers (Wendl et al., 2015). From top: 1) Lomonosovfonna VA (167→152), 2) Lomonosovfonna p-HBA, 3) annual average melt percentage. Gray lines are individual data points. Black lines are 10-year bin averages. The black horizontal lines are the Medieval Climate Anomaly (MCA) and the Little Ice Age (LIA) (Mann et al., 2009). The dashed horizontal line is the extended LIA in the Svalbard region (Divine et al., 2011).

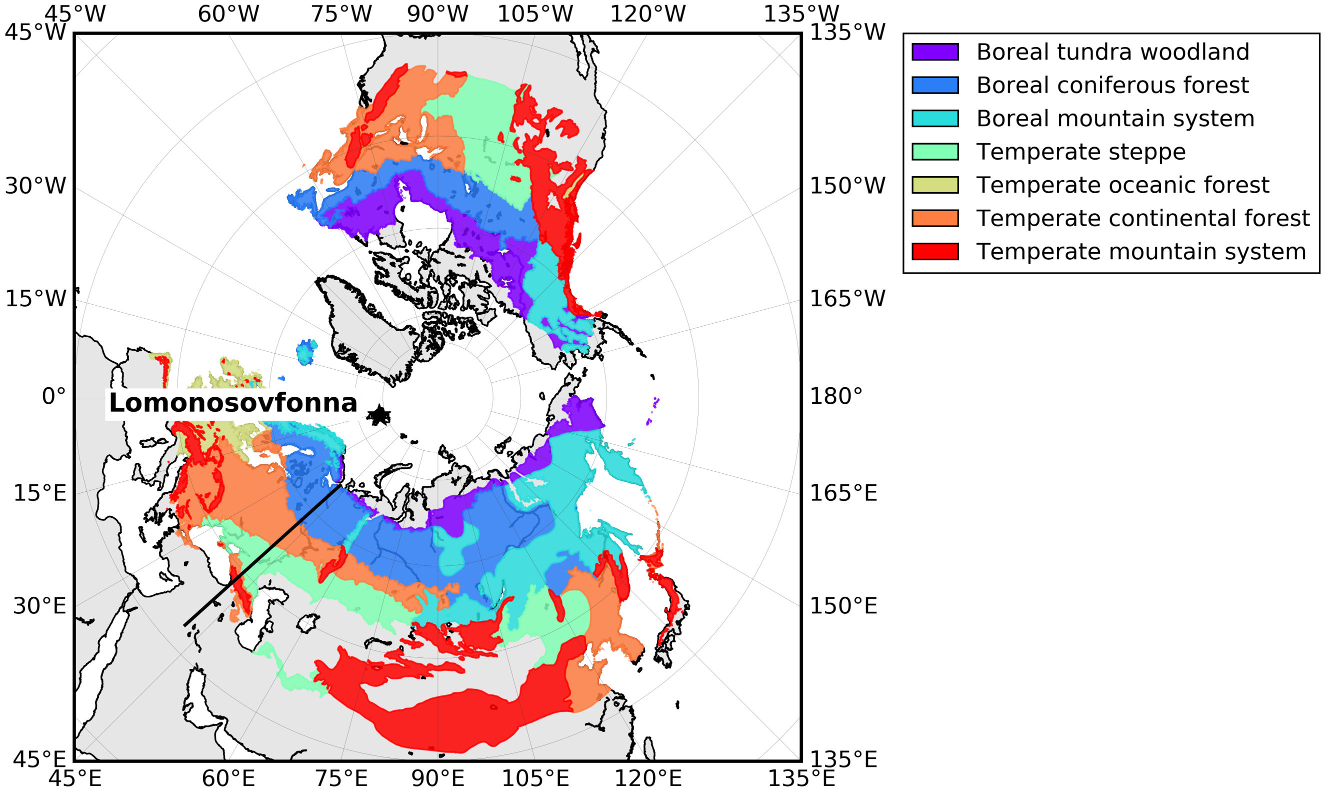

Figure S3. Ecofloristic zones as they are defined by the Food and Agriculture Organization.

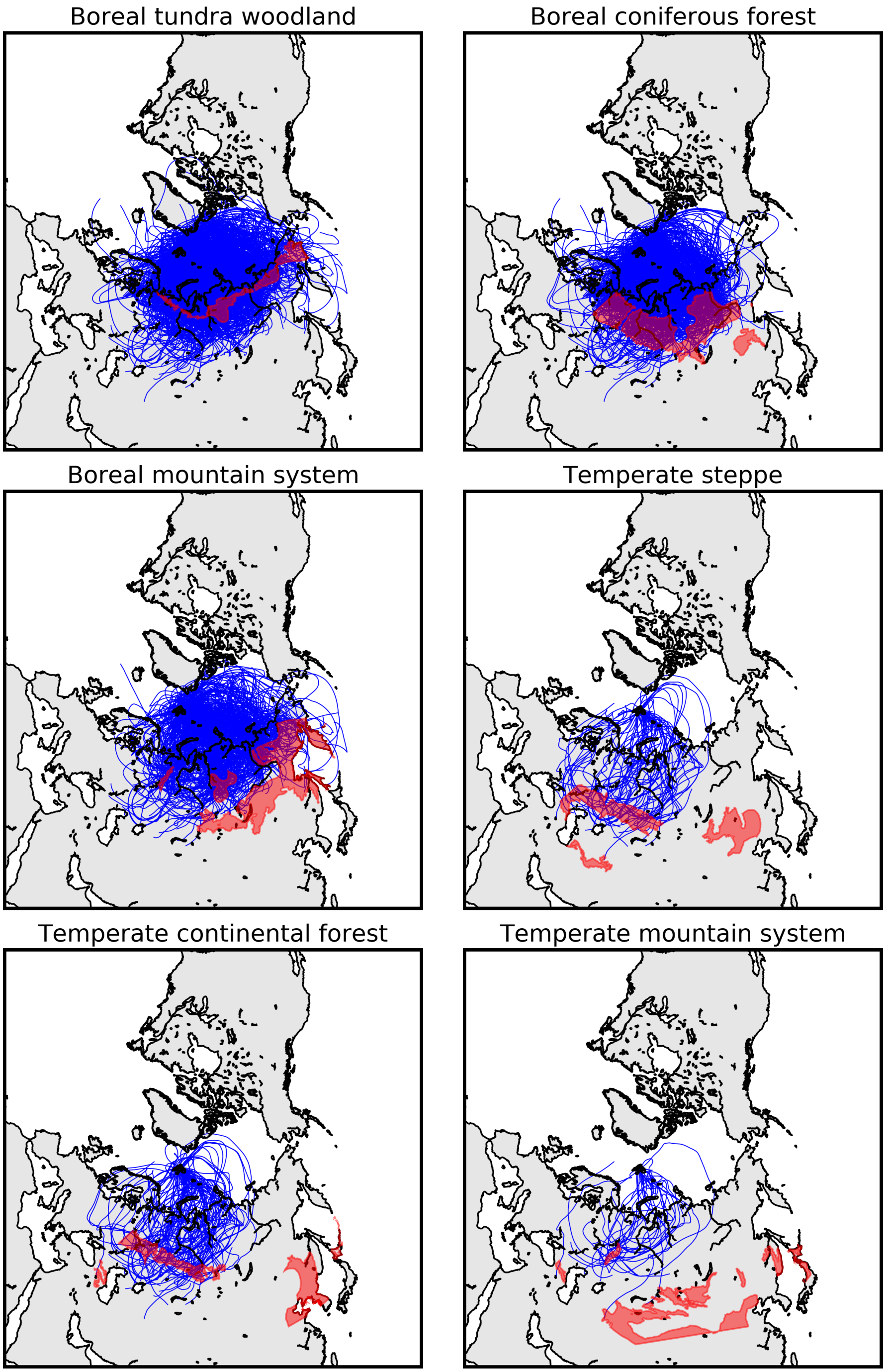

Figure S4. Back trajectories reaching Siberian ecoflorisitic zones. Blue lines are back trajectories reaching the specified ecoflorisitic zones from March-November 2006-2015. Red areas are the ecofloristic zones.

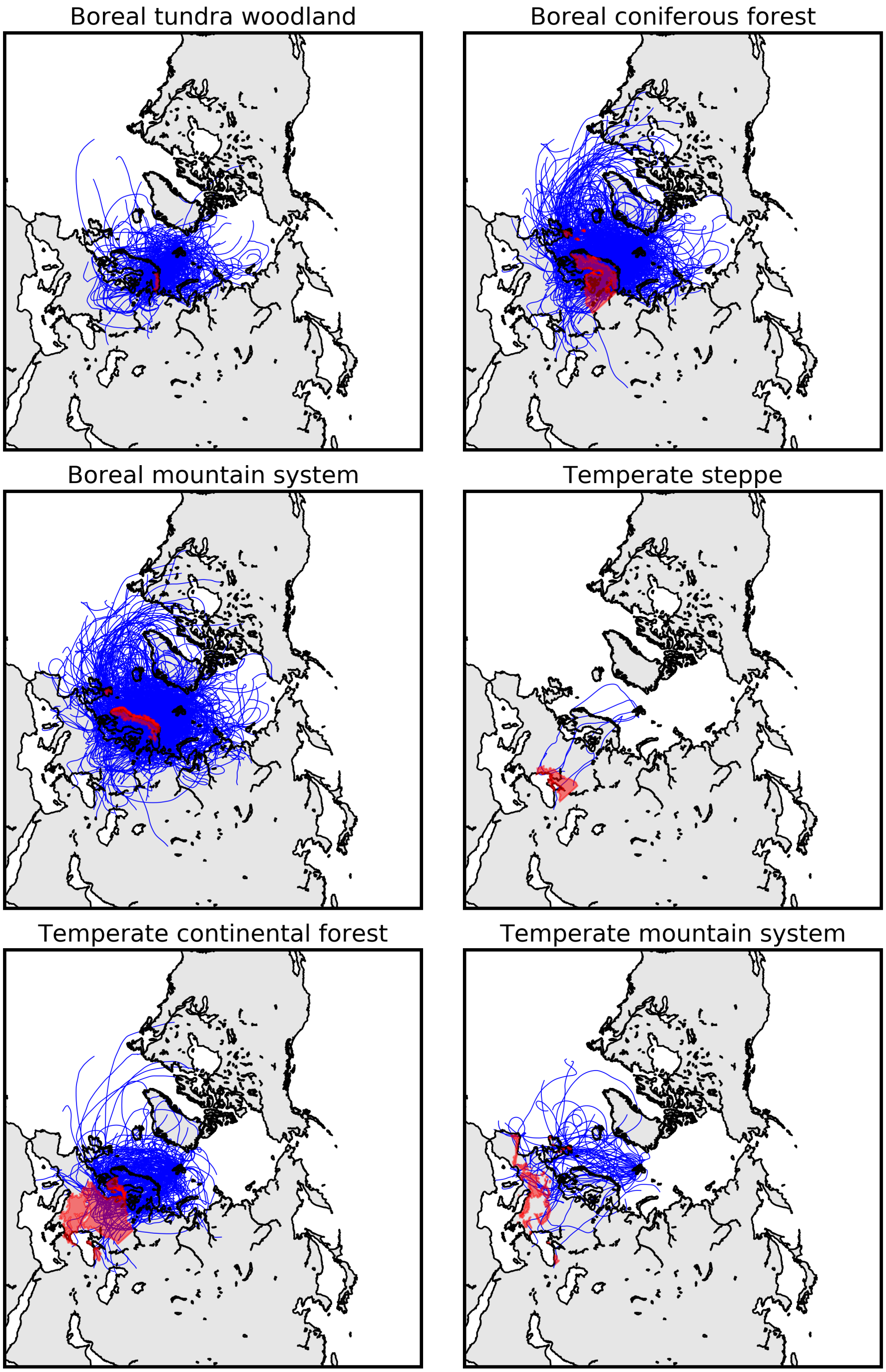

Figure S5. Back trajectories reaching ecoflorisitic zones in Europe. Blue lines are back trajectories reaching the specified ecoflorisitic zones from March-November 2006-2015. Red areas are the ecofloristic zones.

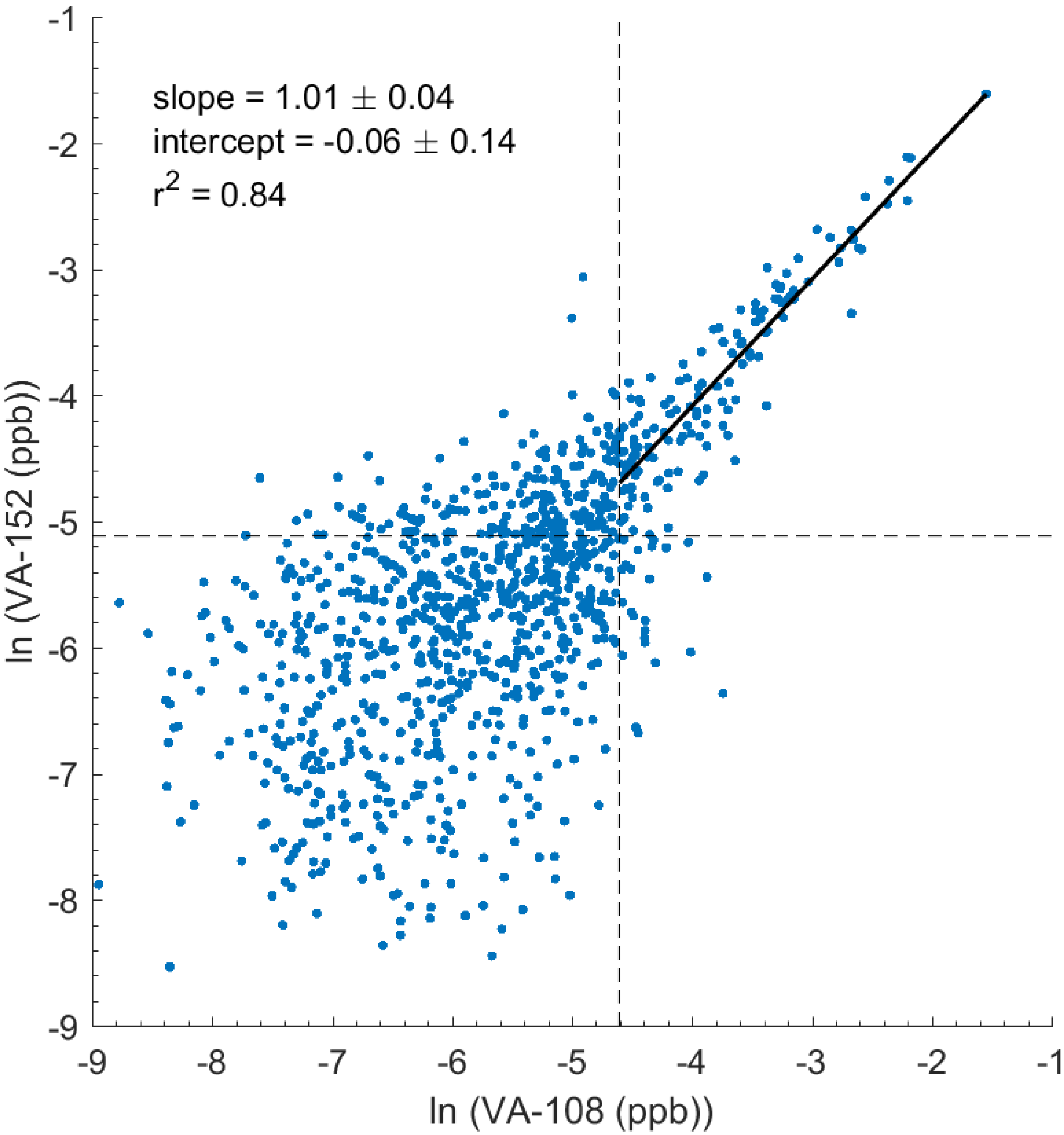

Figure S6. Relationship between two VA mass transitions (m/z 167→108 and 167→152). Black line is the linear fit of the log-transformed data above their respective limits of detection. The dashed lines are the log-transformed limits of detection for each transition.

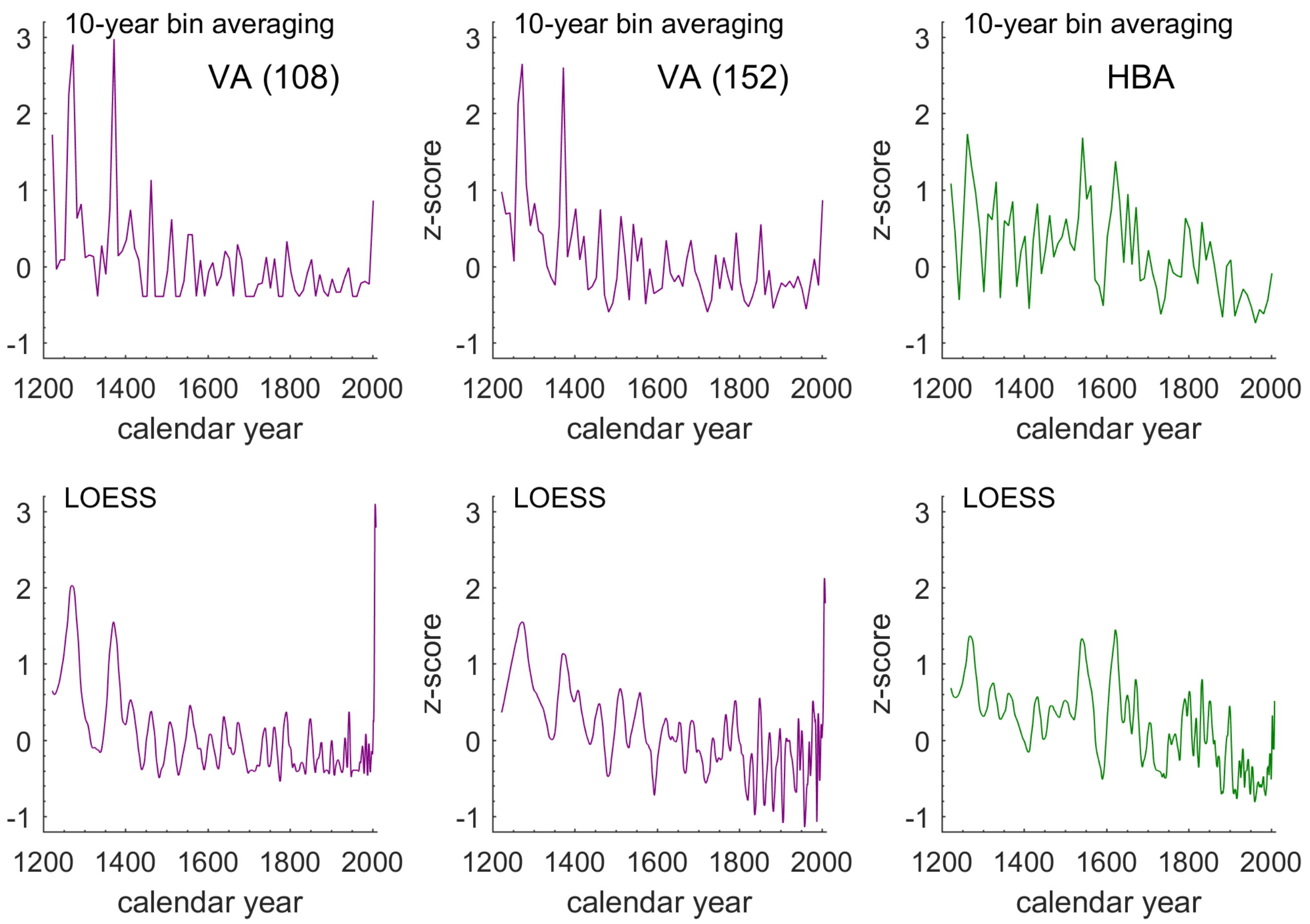

Figure S7. Lomonosovfonna VA (left: m/z 167→108, middle: m/z 167→152) and p-HBA (right) using 10-year bin averaging (top) and LOESS smoothing (span = 0.04) (bottom) of the log transforms. Data were normalized using the mini-max transformation and the z-score.

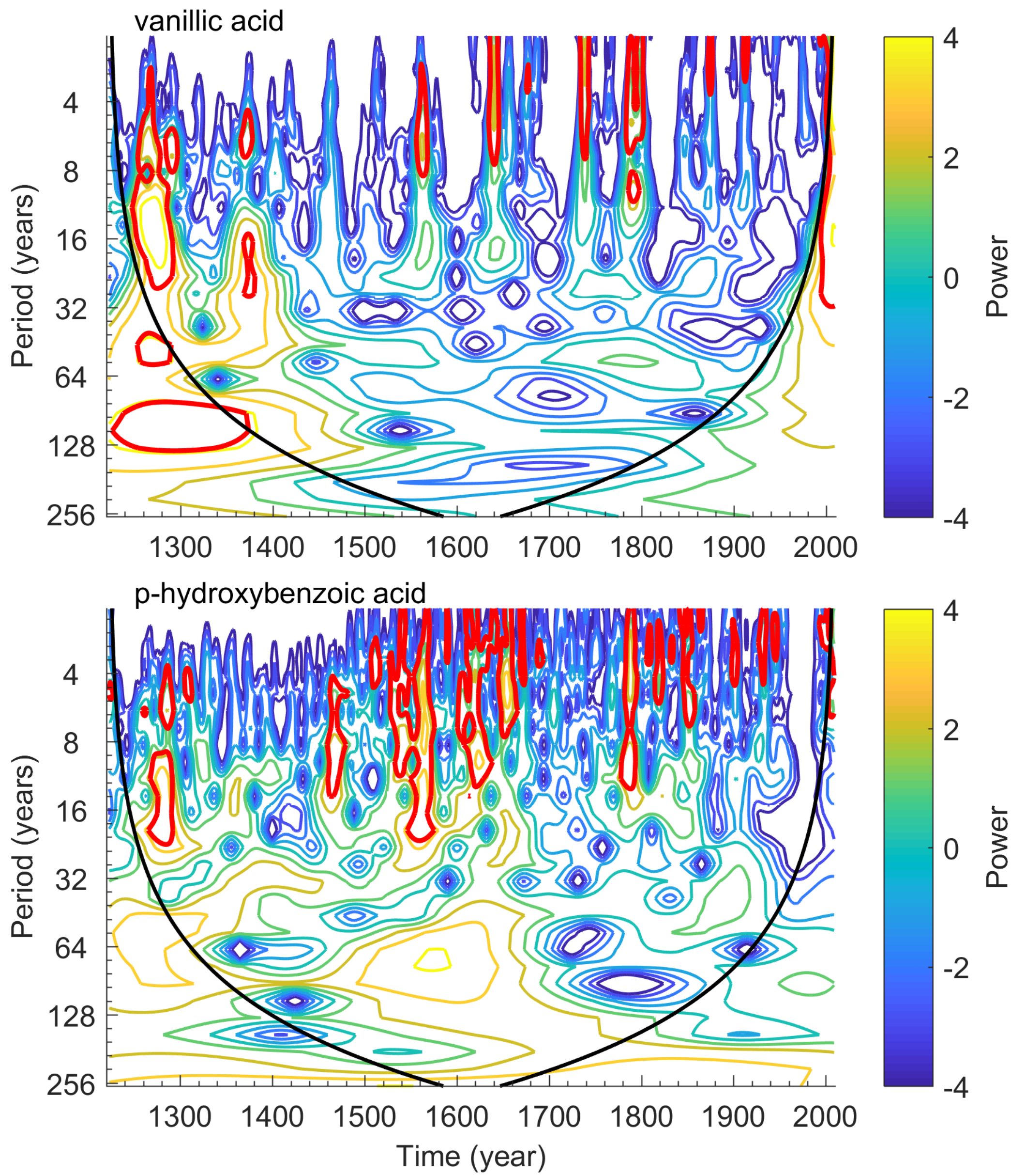

Figure S8. Wavelet analysis of aromatic acids in the Lomonosovfonna, Svalbard ice core: vanillic acid (top) and p-hydroxybenzoic acid (bottom). Black curves are the cones of influence. The red outlines are the 95% confidence interval. Power for wavelet transforms is defined as the logarithm base 2 of the wavelet transform. The continuous wavelet analysis of the data was carried out using MATLAB by interpolating the raw data sets to 1 sample year-1, linear detrending, and applying a Morlet wavelet using the "wavelet" and "wave_signif" functions (Torrence and Compo, 1998). Both VA and p-HBA exhibit peaks in power at ∼100-year and ∼50-year periods early in the record (1200-1400 CE). These peaks are within the 90% confidence interval, but outside of the cone of influence. The VA peak in power at a ∼100-year period decreases until about 1500 CE. The p-HBA peak in power at a ∼100-year period is steady until after 1600 CE. The largest amplitude feature in p-HBA occurs over an 80-100-year period from 1500-1600 CE. This peak in within the 90% confidence interval.

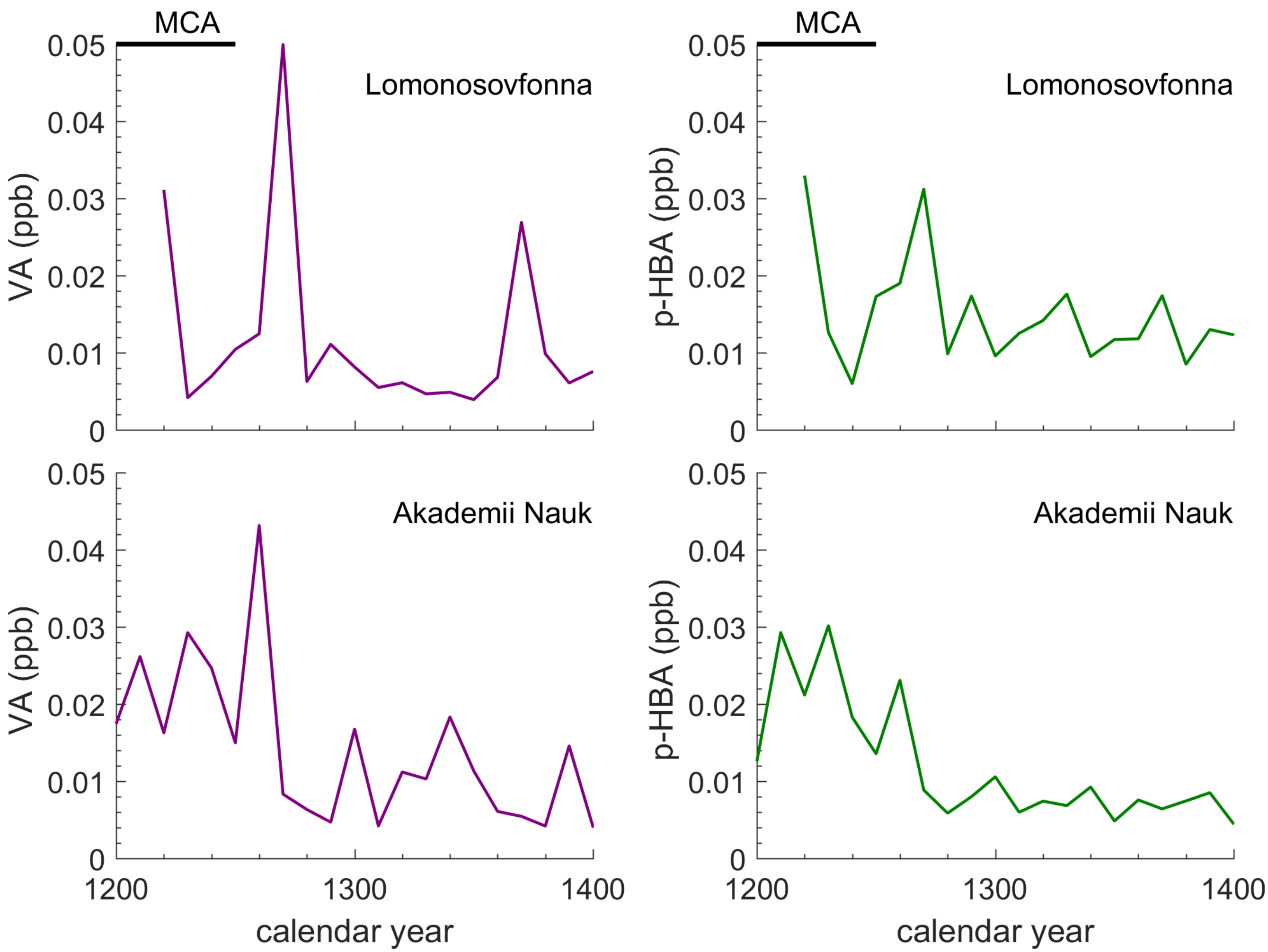

Figure S9. Aromatic acids in the Lomonosovfonna, Svalbard and Akademii Nauk ice cores from 1200-1400 CE. Left: vanillic acid, Right: p-hydroxybenzoic acid. Top: are 10-year bin averages of the Lomonosovfonna ice core measurements. Bottom: 10-year bin averages of the Akademii Nauk ice core measurements (Grieman et al., 2017). The black horizontal lines are the Medieval Climate Anomaly (MCA) (Mann et al., 2009).

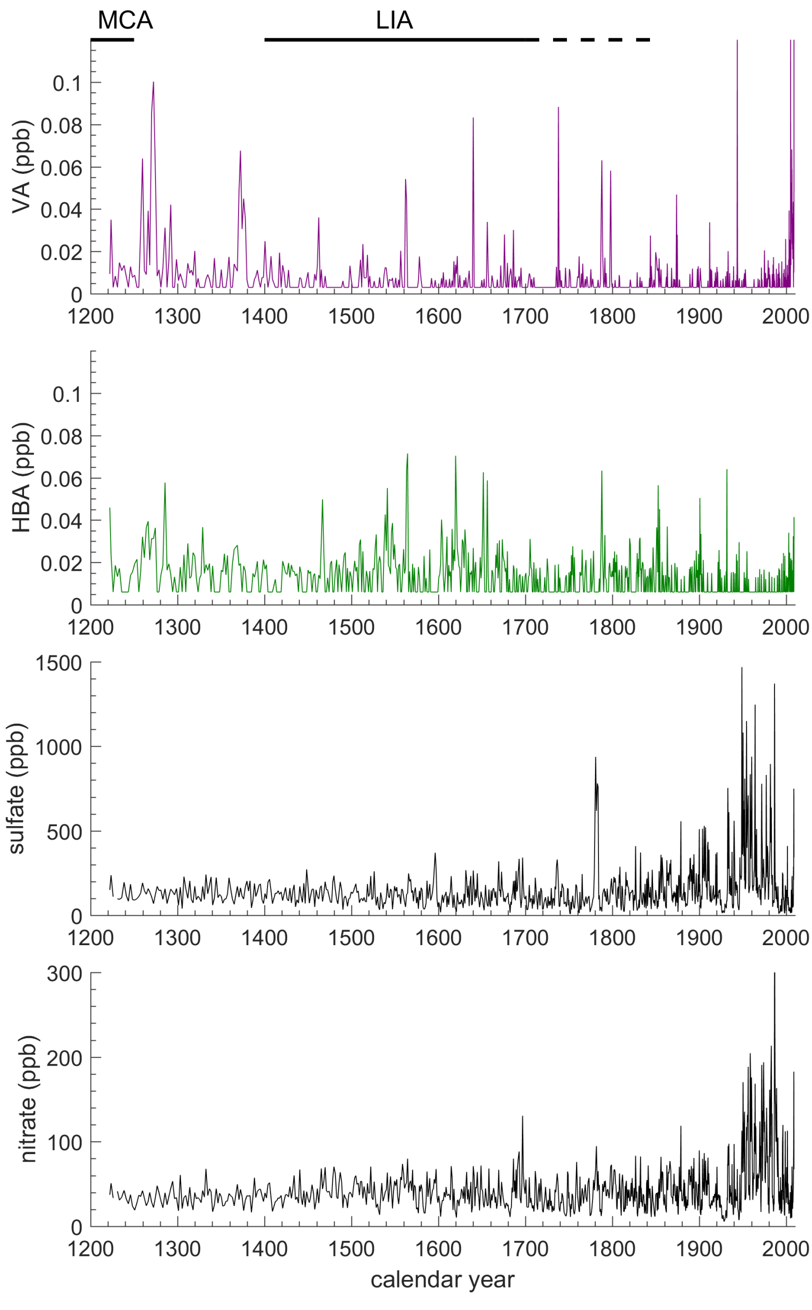

Figure S10. Relationship between Lomonosovfonna vanillic acid, para-hydroxybenzoic acid, nitrate, and sulfate (Wendl et al., 2015). The black horizontal lines are the Medieval Climate Anomaly (MCA) and the Little Ice Age (LIA) (Mann et al., 2009). The dashed horizontal line is the extended LIA in the Svalbard region (Divine et al., 2011).

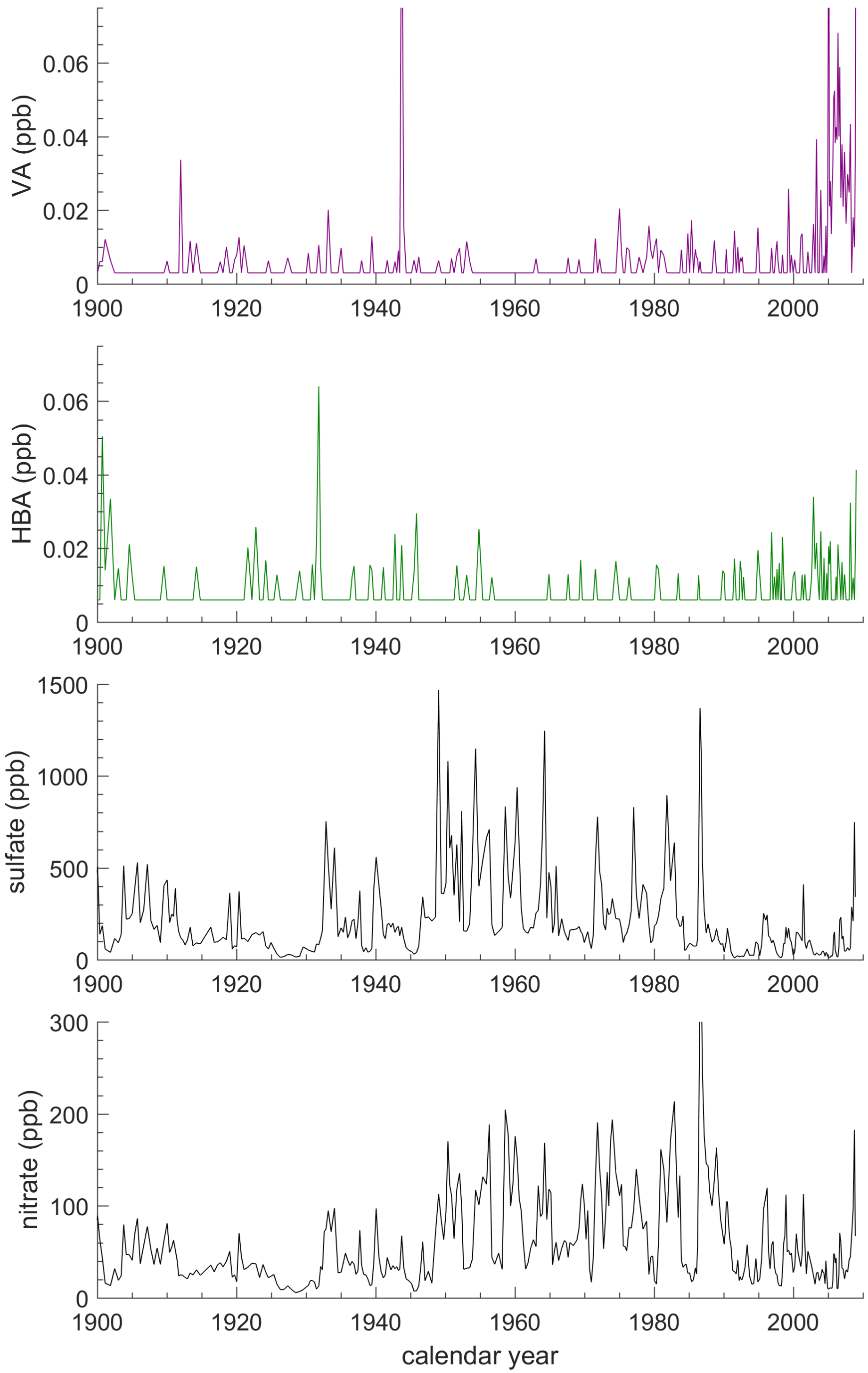

Figure S11. Relationship between Lomonosovfonna vanillic acid, para-hydroxybenzoic acid, nitrate, and sulfate (Wendl et al., 2015) in the 20th century.

Table S1. Fractions of air mass back trajectories transecting or originating from various geographic regions and ecofloristic zones starting from the Lomonosovfonna (Lomo) and Akademii Nauk (AN) drilling sites from 2006-2015 (% rounded to nearest integer). Food and Agriculture Organization definitions of the Ecofloristic zones (Fig. S3; http://cdiac.ornl.gov/epubs/ndp/global_carbon/carbon_documentation.html; Ruesch and Gibbs, 2008). The sum of these values can be >100% if the trajectories transect multiple ecofloristic zones or <100% if trajectories do not reach latitudes below the Arctic. Trajectories commonly do not reach lower latitudes in the summer due to the more northerly position of the Arctic Front relative to the winter (Stohl, 2006).

		Season					
Geographic region	Ecofloristic zone	Spring		Summer		Fall	
		Lomo	AN	Lomo	AN	Lomo	AN
Siberia	Boreal tundra woodland	20	36	5	7	22	40
	Boreal coniferous forest	14	23	3	3	16	32
	Boreal mountain system	9	17	2	2	11	22
	Temperate steppe	2	4	0	0	2	3
	Temperate continental forest	3	5	0	0	2	5
Europe	Boreal tundra woodland	2	1	3	1	3	1
	Boreal coniferous forest	5	1	8	2	8	1
	Boreal mountain system	6	1	10	3	11	2
	Temperate oceanic forest	2	0	4	0	5	1
	Temperate continental forest	2	0	1	0	4	1
North America	Boreal tundra woodland	4	1	2	1	2	0
	Boreal coniferous forest	1	0	1	0	1	0

1 Relationship to sedimentary charcoal records

For comparison to possible biomass burning source regions, charcoal records from two regions, Siberia (12 records, 50-70°N, 50-150°E) and Fennoscandia (19 records, 50-70°N, 0-50°E) were analyzed using the paleofire R package (Global Charcoal Database accessed at: http://gpwg.paleofire.org; Blarquez et al., 2014). Only 3 of the 12 Siberian records have enough data from 1200-2000 CE for comparison to the Lomonosvfonna ice core record. These regions are Chai-ku Lake in eastern Siberia, and Zagas Nuur and Lake Teletskoye in southern Siberia. The Siberian region as a whole is therefore not well-represented. Only 6 of the 19 Fennoscandian records have enough data from 1200-2000 CE for comparison to the Lomonosovfonna ice core record. Siberia and Fennoscandia are primarily boreal tundra woodlands, boreal conifer forests, and boreal mountain systems (Fig. S3; Ruesch and Gibbs, 2008). One important caveat to this comparison is that the dating of sedimentary charcoal records is often based on linear interpolations between a few ^{14}C ages. Hence their age scales are typically less well constrained than Lomonosovfonna or other ice cores.

Four of the six records from Fennoscandia exhibit increased charcoal influx from 1200-1400 CE (Fig. S11; Blarquez et al., 2014). Lomosovfonna VA and p-HBA are both elevated during this period. Three of the six charcoal records are elevated around 1600 CE when Lomonosovfonna p-HBA is also elevated. Two of the records also show a long-term decline from 1200-2000 CE similar to the Lomosovfonna VA and p-HBA records. There are relatively few Siberian charcoal records in the Global Charcoal Database (http://gpwg.paleofire.org; Blarquez et al., 2014). Two of the Siberian records exhibited increased charcoal influx from 1200-1600 CE relative to 1600 CE to present (Fig. S12). The Lomonosovfonna VA and p-HBA are also higher early in the record. It is not possible to determine the source location of the VA and the p-HBA in the Lomonosovfoanna from so few charcoal records. The Fennoscandian records are clearly most similar to the Svalbard ice core record.

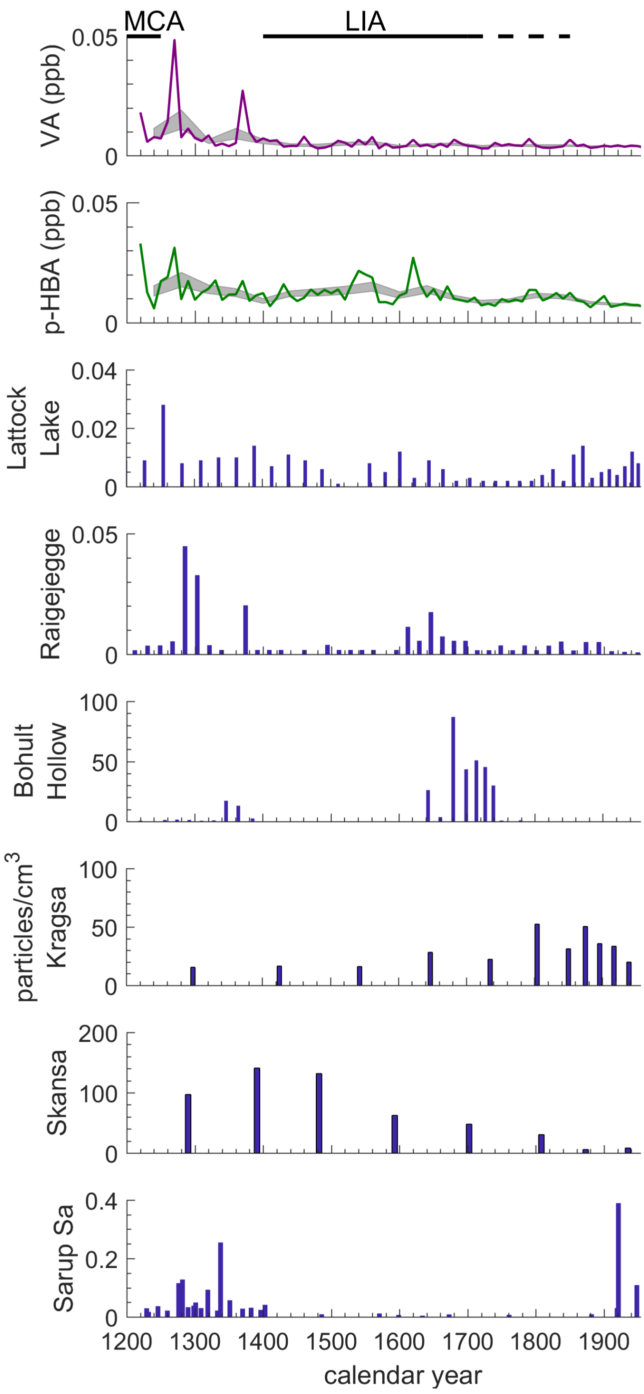

Figure S12. Comparison of the timing of aromatic acid signals in the Lomonosovfonna ice core over the past 800 years compared to Fennoscandia charcoal records. From top: 10-year bin averages of Lomonosovfonna vanillic acid (VA) and p-hydroxybenzoic acid (p-HBA); and charcoal influx records from Lattock Lake, Raigejegge, Bohult Hollow, Skansa, and Sarup Sa (Blarquez et al., 2014). The black horizontal lines are the Medieval Climate Anomaly (MCA) and the Little Ice Age (LIA) (Mann et al., 2009). The dashed horizontal line is the extended LIA in the Svalbard region (Divine et al., 2011).

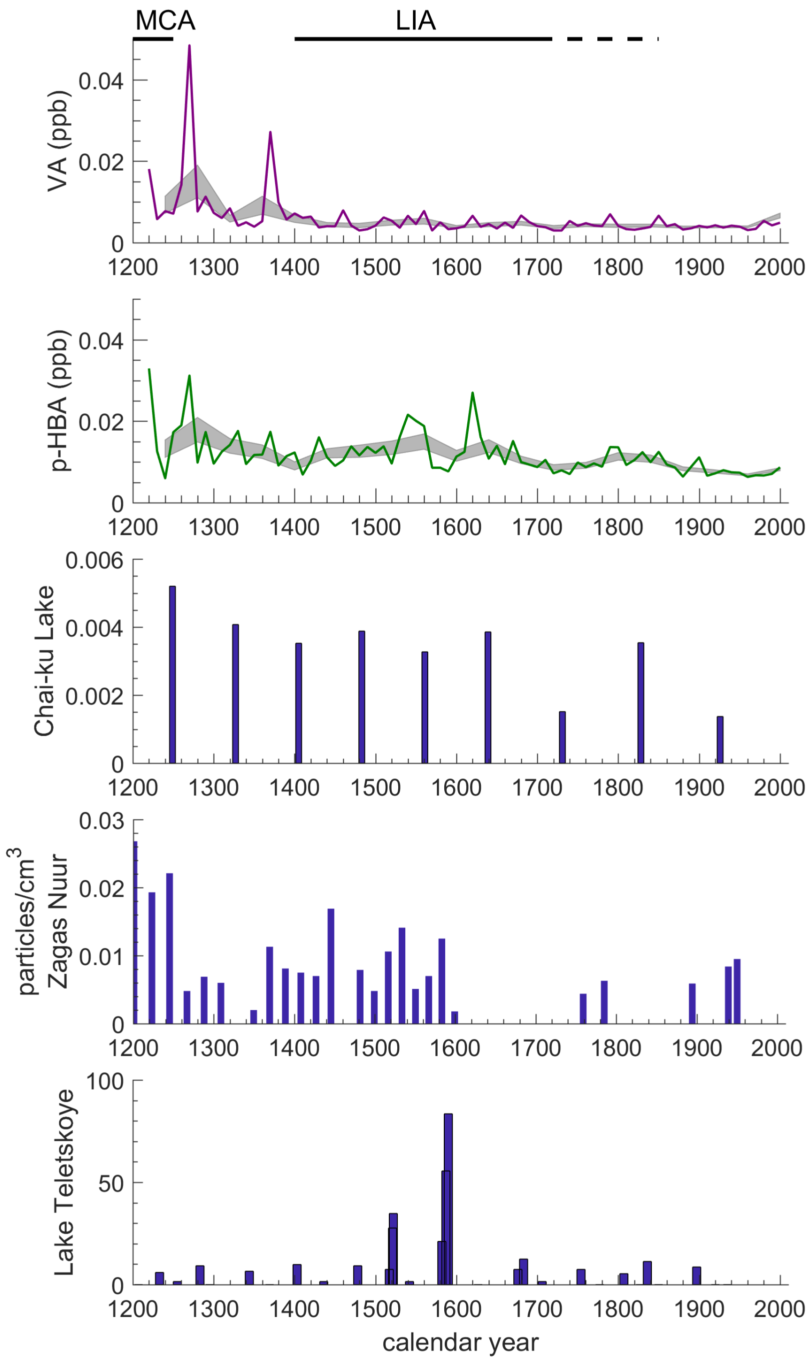

Figure S13. Comparison of the timing of aromatic acid signals in the Lomonosovfonna ice core over the past 800 years compared to Siberian charcoal records. From top: 10-year bin averages of Lomonosovfonna vanillic acid (VA) and p-hydroxybenzoic acid (p-HBA); and charcoal influx records from Chai-ku Lake, Zagas Nuur, and Lake Teletskoye (Blarquez et al., 2014). The black horizontal lines are the Medieval Climate Anomaly (MCA) and the Little Ice Age (LIA) (Mann et al., 2009). The dashed horizontal line is the extended LIA in the Svalbard region (Divine et al., 2011).

References

Blarquez, O., Vannière, B., Marlon, J. R., Daniau, A.-L., Power, M. J., Brewer, S., and Bartlein, P. J.: Paleofire: An R package to analyse sedimentary charcoal records from the Global Charcoal Database to reconstruct past biomass burning, Computers and Geosciences, 72, 255 – 261, doi:10.1016/j.cageo.2014.07.020, 2014.

Divine, D., Isaksson, E., Martma, T., Meijer, H. A., Moore, J., Pohjola, V., van de Wal, R. S. W., and Godtliebsen, F.: Thousand years of winter surface air temperature variations in Svalbard and northern Norway reconstructed from ice-core data, Polar Research, 30, 7379, doi:10.3402/polar.v30i0.7379, 2011.

Grieman, M. M., Aydin, M., Fritzsche, D., McConnell, J. R., Opel, T., Sigl, M., and Saltzman, E. S.: Aromatic acids in a Eurasian Arctic ice core: a 2600-year proxy record of biomass burning, Climate of the Past, 13, 395–410, doi:10.5194/cp-13-395-2017, 2017.

Mann, M. E., Zhang, Z., Rutherford, S., Bradley, R. S., Hughes, M. K., Shindell, D., Ammann, C., Faluvegi, G., and Ni, F.: Global Signatures and Dynamical Origins of the Little Ice Age and Medieval Climate Anomaly, Science, 326, 1256–1260, doi:10.1126/science.1177303, 2009.

Ruesch, A. and Gibbs, H. K.: New IPCC Tier-1 global biomass carbon map for the year 2000, Carbon Dioxide Information Analysis Center, Oak Ridge National Laboratory, 2008.

Stohl, A.: Characteristics of atmospheric transport into the Arctic troposphere, Journal of Geophysical Research: Atmospheres, 111, doi:10.1029/2005JD006888, 2006.

Torrence, C. and Compo, G. P.: A practical guide to wavelet analysis, Bulletin of the American Meteorological society, 79, 61–78, doi:10.1175/1520-0477(1998)079<0061:APGTWA>2.0.CO;2, 1998.

Wendl, I., Eichler, A., Isaksson, E., Martma, T., and Schwikowski, M.: 800-year ice-core record of nitrogen deposition in Svalbard linked to ocean productivity and biogenic emissions, Atmospheric Chemistry and Physics, 15, 7287–7300, 2015.